CLAS-ANALYSIS NOTE

Dalitz Plot Analysis of $\eta' \to \eta\ \pi^+\ \pi^-$ from CLAS G12 Data Set

1. Introduction

The present work aims to report the Dalitz plot parameters for $\eta' \to \eta\ \pi^+\ \pi^-$ decay. The three body decay of a meson has two degrees of freedom, so one can define a Dalitz plot with two variables X and Y for $\eta' \to \eta\ \pi^+\ \pi^-$ decay, which is defined as follows:

$$X = \frac{\sqrt{3}(T_{\pi^+} - T_{\pi^-})}{Q} \tag{1}$$

$$Y = \frac{(m_\eta + 2m_\pi)}{m_\pi} \cdot \frac{T_\eta}{Q} - 1. \tag{2}$$

Where T_η, T_{π^+} and T_{π^-} are the kinetic energy of a given particles η, π^+ and π^- respectively in the rest frame of η' and Q = T_{π^+}+T_{π^-}+T_η. The m_η and m_π are the mass of η and π mesons respectively.

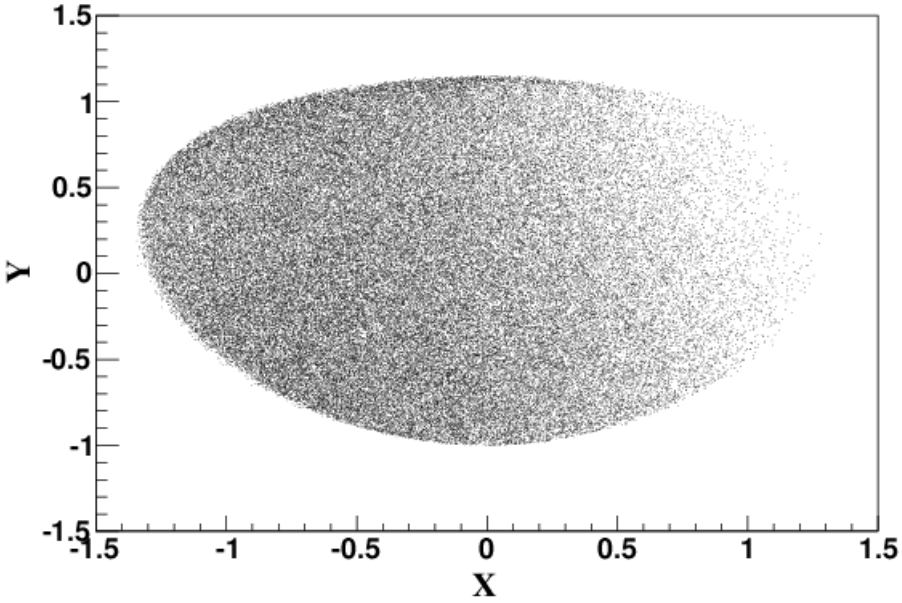

FIGURE 1. Dalitz variable X vs Y for $\eta' \to \eta\ \pi^+\ \pi^-$.

The general parametization function in Equation. 6 is used to fit a Dalitz plot. The square of the decay amplitude,

$$M^2 = A(1 + aY + bY^2 + cX + dX^2). \tag{3}$$

Where a, b, c, and d are the Dalitz plot parameters of the decay and A is the normalization constant.

The Dalitz plot(DP) provides pure kinematic information of a three body decay and also helps to understand the correct input to theoretical distribution of the effective chiral Lagrangian. A Dalitz plot study for the η' meson for the $\eta\ \pi^+\ \pi^-$ decay channel will help to study effective chiral perturbation theory at a low Q limit.

The VES Collaboration has reported the Dalitz plot parameters of $\eta' \to \eta\ \pi^+\ \pi^-$ with 14.6 x 10^3 events in charge exchange and 7 x 10^3 events in diffraction like production [1]. The BESIII Collaboration has also reported $\eta' \to \eta\ \pi^+\ \pi^-$ decay parameters with 43826 211 events with better precision [2]. The two measurements has disagreement among them and also to the theoretical calculation of the parameters [3].

In this note the Dalitz plot parameters of $\eta' \to \eta\ \pi^+\ \pi^-$ is studied with CLAS g12 data set, which has the competitive statistics to study the parameters with low statistical errors. It is yet another independent measurement with different systematic errors to cross-check the parameters.

2. G12 Data Set

The g12 experiment ran during March - June 2008 with 26 x 10^9 recorded production triggers [4]. The fixed target g12 experiment, has an energy of the photon beam ranging from 1.142 GeV to 5.425 GeV. However the threshold production of η' meson is 1.455 GeV and hence the analysis will report the parameters from the threshold to the maximum available energy. The analysis starts with well calibrated data in ".root" format with all events arranged as per the Run number, Event number and PID along with all other informations recorded by the experiment. The final state particles proton, π^+ and π^- information were extracted from the PART BOS bank and identified using particle identification codes compiled in the "clas6-trunk" under the package CLASEVENT . The skim were so selected that all events has only one proton, π^+ and π^- and any number of

neutral particles. The complete reaction under study is " γ p $\rightarrow \eta'(\rightarrow \eta\ \pi^+\ \pi^-)$ p " and the η meson is detected via the missing mass technique.

2.1. Run List

The g12 experiment recorded 626 production runs, 37 single-prong runs and 3 special calibration runs. The Table. 1 shows the list of runs used in the analysis.

TABLE 1. List of runs included in the analysis

G12 Run List	G12 Run List	G12 Run List	G12 Run List	G12 Run List
56605	56653	56654	56655	56656
56660	56661	56665	56666	56667
56668	56669	56670	56673	56674
56688	56689	56690	56691	56692
56693	56694	56695	56696	56700
56701	56702	56703	56704	56705
56706	56707	56708	56710	56711
56712	56713	56714	56715	56716
56717	56718	56719	56720	56721
56722	56723	56724	56726	56727
56728	56729	56730	56731	56732
56733	56734	56735	56736	56737
56738	56739	56740	56741	56742
56743	56744	56748	56749	56750
56751	56752	56753	56754	56755
56756	56757	56758	56759	56760
56761	56762	56763	56764	56765
56766	56767	56768	56770	56771
56772	56774	56775	56776	56777
56778	56780	56781	56782	56783
56784	56787	56788	56791	56792

56793	56794	56798	56799	56800
56801	56802	56805	56806	56807
56808	56809	56810	56811	56812
56813	56814	56815	56821	56822
56823	56824	56825	56826	56827
56831	56832	56833	56834	56838
56839	56841	56842	56843	56844
56845	56849	56853	56854	56855
56856	56857	56858	56859	56860
56861	56862	56864	56865	56866
56870	56874	56875	56877	56879
56897	56898	56899	56900	56901
56902	56903	56904	56905	56907
56908	56914	56915	56916	56917
56918	56919	56921	56922	56923
56924	56925	56926	56927	56928
56929	56930	56932	56935	56936
56937	56938	56939	56940	56948
56949	56950	56951	56952	56953
56954	56955	56956	56958	56960
56961	56962	56963	56964	56965
56966	56967	56968	56969	56970
56971	56972	56973	56974	56975
56977	56978	56979	56980	56992
56993	56994	56996	56997	56998
56999	57000	57001	57002	57003
57004	57005	57006	57008	57009
57010	57011	57012	57013	57014
57015	57016	57017	57021	57022
57023	57025	57026	57027	57030

57031	57032	57062	57063	57064
57065	57066	57067	57068	57069
57071	57072	57073	57075	57076
57077	57078	57079	57080	57095
57096	57097	57100	57101	57102
57103	57106	57107	57108	57114
57115	57116	57117	57118	57119
57120	57121	57122	57123	57124
57125	57126	57127	57128	57130
57131	57132	57133	57134	57135
57136	57137	57138	57139	57140
57141	57142	57143	57144	57145
57146	57147	57148	57149	57150
57151	57152	57159	57160	57161
57162	57163	57164	57165	57166
57167	57168	57170	57171	57172
57173	57174	57175	57176	57177
57178	57179	57180	57181	57182
57183	57184	57185	57189	57190
57191	57192	57193	57194	57195
57196	57197	57198	57199	57200
57201	57202	57203	57204	57205
57206	57207	57208	57209	57210
57211	57212	57213	57214	57215
57216	57217	57218	57219	57220
57221	57222	57223	57224	57225
57226	57227	57228	57229	57233
57234	57235	57236	57249	57250
57251	57252	57253	57255	57256
57257	57258	57260	57261	57262

57263	57264	57265	57266	57267
57268	57270	57271	57272	57274
57275	57276	57277	57278	57279
57280	57281	57282	57283	57284
57285	57286	57287	57288	57290
57291	57293	57294	57295	57296
57297	57298	57299	57300	57301
57302	57303	57304	57305	57306
57307	57308	57309	57310	57311
57317	57308	57309	57310	57311

The whole analysis is divided into following sections.

- Simulation
- Event Selection
- Result
- Systematics Study

2.2. Simulation

PLUTO++, an event generator is used for this analysis. It uses ROOT based programmes and it is very commonly used in Hadron Physics experiments to generate hadronic production and decay of mesons. It gives user the freedom to include physics models with simple C++ based codes and to obtain outputs in any desired format. The simulated events in the analysis are modelled with bremsstrahlung photon, differential cross-section of η' and Dalitz plot parameters of $\eta' \rightarrow \eta\ \pi^+\ \pi^-$ decay. The output of the PLUTO++ program are extracted in standard CLAS "gamp" file and then processed with CLAS simulation suit in the following way :

- The gamp files are first converted into the format of PART bank containing the event.
- GSIM: Geant3-based simulation in CLAS simulates the decay tracks of particles through the simulation and finally the digitized informations is sorted in the simulated "raw" banks.
- GPP: GSIM post-processor smears detector signal more accurately to reflect the actual resolution and to simulate the experimental conditions.
- a1c : It is used for reconstruction of simulated data and is the same program used during data reconstruction.

3. Event Selection

This section explains the procedure to improve the identification of the particles, corrections to the event and cuts to the analysis.

3.1. Selection of the Beam Photon

A typical g12 data event has multiple bremsstrahlung photons recorded as the incident beam. The multiple beam photon arises from 2.004 beam bunching spacing of the electrons in the storage ring. These electrons gives the bremsstrahlung photons in the radiator and creates multiple hits in the trigger and thereby satisfying trigger logic to record them. All the photons which falls within the timing window of |Tagger Time - StartTime| $\leq$ 1.002 ns are considered as an individual event.

3.2. G12 Corrections

The G12 Corrections were derived from the exclusive π^+, π^- and proton reaction. We used the following corrections in the analysis [4]:

- Beam Energy Correction : Is a correction to the incident beam photon energy and dependent on the Run number of the event. This correction is only applicable data and not to the simulated events.
- Removal of bad TOF paddle : This correction takes the Sector number and Paddle number as input. We used the correction to remove only those paddles that shows a significant drift on the resolutions of particle.
- Geometric Fiducial Cut : This cut removes the dead part of the detector from the $\theta - \phi$ map of the particle. We used it with the "nominal" option.

3.3. Kinematic Fitting

Kinematic fitter is a useful tool often used to get rid of unwanted background from signal channels and helps to improve the signal to background ratio. Any measurement with a tool comes with an error, and it can be represented as a vector $\vec{\eta}$. We can also define the measurement as

$\vec{\eta} = \vec{y}. + \vec{\epsilon}.$

Where the $\vec{y}$ and $\vec{\epsilon}$ denotes the actual value of the measurement without error and $\vec{\epsilon}$ is the error associated with the measurement. The kinematic information of a physics channel along with the constrains imposed allows the fitter to calculate the probability and χ^2 of each event using Lagrange multipliers to perform a least-squares fit. The CLAS g12 Kinematic fitter takes the "TBER (Track Based Error)" matrix, vertex of information and four-momentum of all particles as input, and returns Pull probabilities and χ^2 for each events. The Pull probabilities when fitted with Guassian, its mean and σ decides the quality of the covariance matrix and kinematic fit. In the ideal case of gaussian fitted to the Pulls of the particles should have zero mean and σ of one, which ensures that the fitter correctly calculates covariance matrix error.

The CLAS g12 Kinematic fitter is tuned for 4C constrained reaction,

$$\gamma p \rightarrow \pi^+ \pi^- p.$$

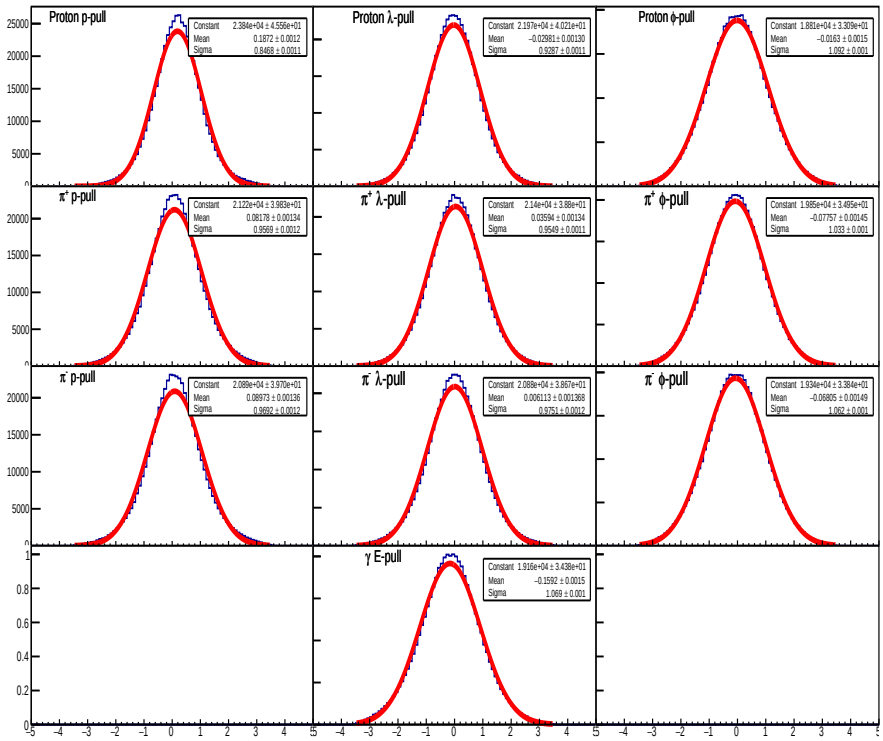

FIGURE 2. The Pull distributions for a (4-C) kinematic fit to γ p $\rightarrow$ π^+ π^- p from g12 data with run 56655 after a 1% Pull probability cut.

The tuning were done for π^+ π^- and p individually. To check the quality of covariance matrix the mean and sigma of the tuned pulls of the particles π^+, π^- and p from the reaction hypothesis for the data with run 56655 and simulation after a 1% pull probability cut is listed in the Table. 2.

3.3.1. *Kinematic Fit to the Analysis.* The tuned Kinematic fitter for the 4C constrained fit is again used for the channel below

$$\gamma p \rightarrow (\eta)_{Missing}\pi^+\pi^- p.(1-C)$$

The 1-C constrained fit requires the four-momentum [beam] + [target] - ([π^+] [π^-] [p]) to be an [η] meson. The reaction hypothesis has the same set of final state particles as for the tuned channel, hence one can comfortably use it without tuning it for our reaction

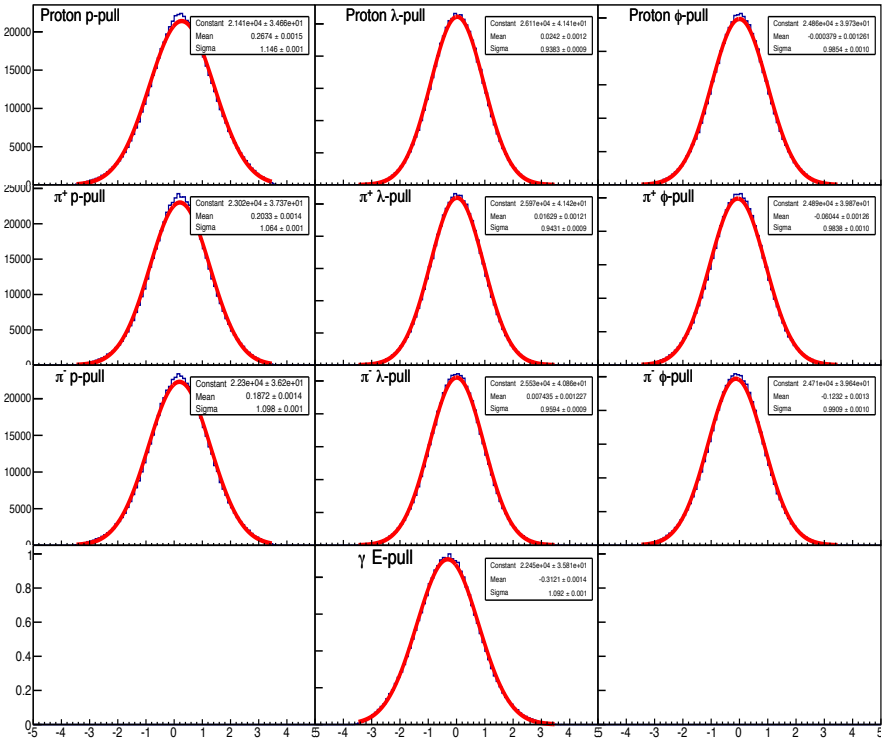

FIGURE 3. The Pull distributions for a (4-C) kinematic fit to γ p $\rightarrow$ π^+ π^- p from g12 simulation after a 1% Pull probability cut.

hypothesis again. The Pull probability for the channel is shown in Fig. 4 and the dotted line at 0.01 shows the 1% Pull probability cut to reject events.

3.4. $\mid \cos\theta_{center-of-mass}$ of $\eta' \mid \leq$ 0.85 Cut

The events are generated with the differential cross sections of η' from the g11 measurement [5] within a $\mid \cos\theta_{center-of-mass}$ of $\eta' \mid \leq 0.85$. The earlier measurement of CLAS g11 has reported the differential cross sections in $\mid \cos\theta_{center-of-mass}$ of $\eta' \mid \leq 0.85$ window as the yield drops near to the beam pipe and hence this region is removed from the analysis.

3.5. $\mid \cos\theta_{center-of-mass}$ of $\eta \mid \leq$ 0.85 Cut

The η mesons along the beam pipe in the forward and backward region is removed with a condition requiring $\mid \cos\theta_{center-of-mass}$ of $\eta \mid \leq 0.85$. The Figure. 5 shows the

(A)

	μ	σ
Proton p-pull	0.187	0.846
Proton λ-pull	-0.029	0.928
Proton ϕ-pull	-0.016	1.092
π^+ p-pull	0.081	0.957
π^+ λ-pull	0.035	0.954
π^- ϕ-pull	-0.077	1.033
π^- p-pull	0.089	0.969
π^- λ-pull	0.006	0.975
π^- ϕ-pull	-0.068	1.062
γ E-pull	-0.159	1.069

(B)

	μ	σ
Proton p-pull	0.267	1.146
Proton λ-pull	0.024	0.938
Proton ϕ-pull	-0.000	0.985
π^+ p-pull	0.203	1.064
π^+ λ-pull	0.016	0.943
π^+ ϕ-pull	-0.060	0.983
π^- p-pull	0.187	1.098
π^- λ-pull	0.007	0.959
π^- ϕ-pull	-0.123	0.990
γ E-pull	-0.312	1.092

TABLE 2. The table shows the Gaussian mean (μ) and width (σ) for the pull distributions from a 4C kinematic fit of γ p $\rightarrow$ π^+ π^- to events from (A) data run 56655 and (B) from simulation after a 1% Pull probability cut.

cos(θ) distribution of η meson in the rest frame of η' meson for both data and simulation. The Figure. 6 clearly shows the steep drop of acceptance for the η meson with high kinetic energy decaying along the beam pipe region. Hence the a geometrical cut at $\mid \cos \theta_{center-of-mass}$ of $\eta \mid \leq 0.85$ is placed in order to calculate integrated acceptance for Dalitz plot parameters.

The kinematics of η meson is directly related to the Dalitz variable Y. Hence a comparison of the cut is also presented for the Dalitz variable Y in Figure. 7 and 8 from simulation and g12 data respectively.

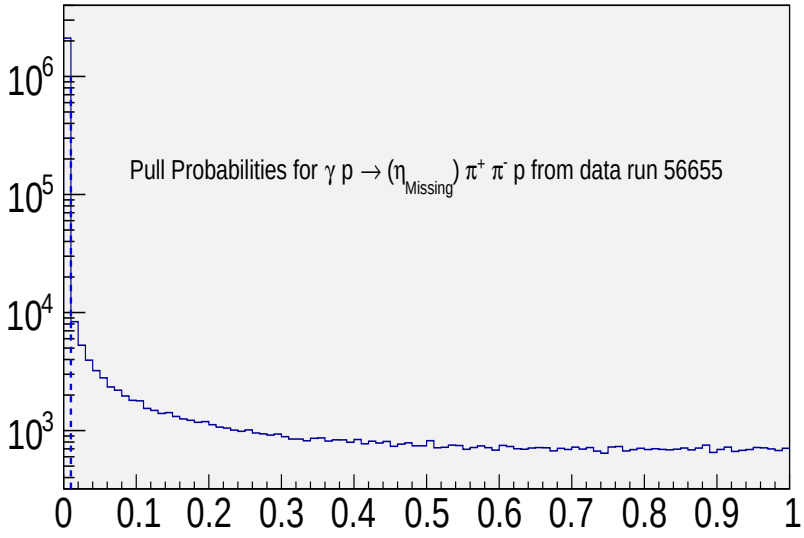

FIGURE 4. The Pull probability for a (1-C) kinematic fit to γ p $\rightarrow$ ($\eta_{Missing}$) π^+ π^- p from data run 56655.

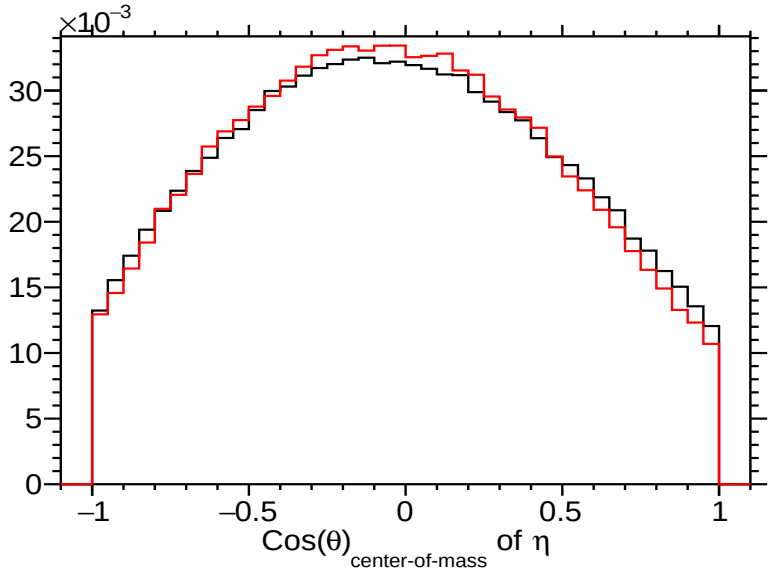

FIGURE 5. $\cos\theta_{center-of-mass}$ of η distribution from g12 data and simulation.

3.6. Vetex Cut

In the g12 experiment the target was positioned -90 cm from the CLAS center. The target cell was 40 cm long and 2 cm in radius in the form of a cylinder filled with unpolarised liquid hydrogen. We used this target information and imposed it to all event

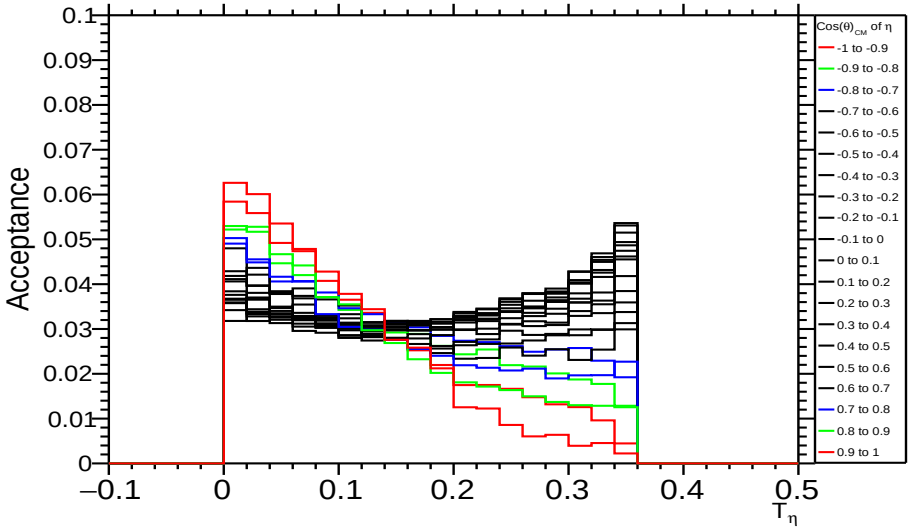

FIGURE 6. The acceptance vs T_η in 0.1 bins of cos $\theta_{center-of-mass}$ of η meson.

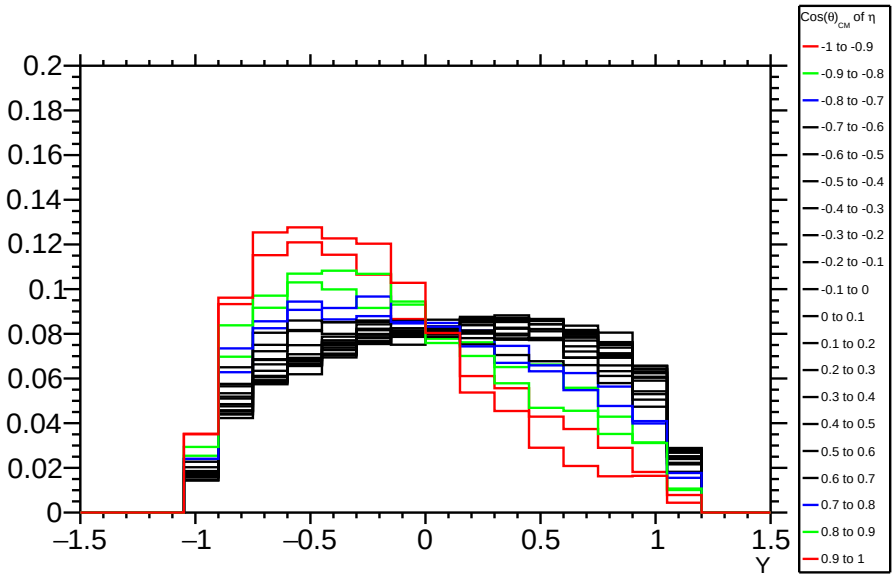

FIGURE 7. Dalitz Variable Y distribution normalised to 1 in each 0.1 bins of cos $\theta_{center-of-mass}$ of η from simulation.

vertexes. We required all events production vertex tracks to originate in the target region via the condition that $\sqrt{v_x^2 + v_y^2} \leq 2$ cm and -110 $\geq v_z \leq$ -70 cm.

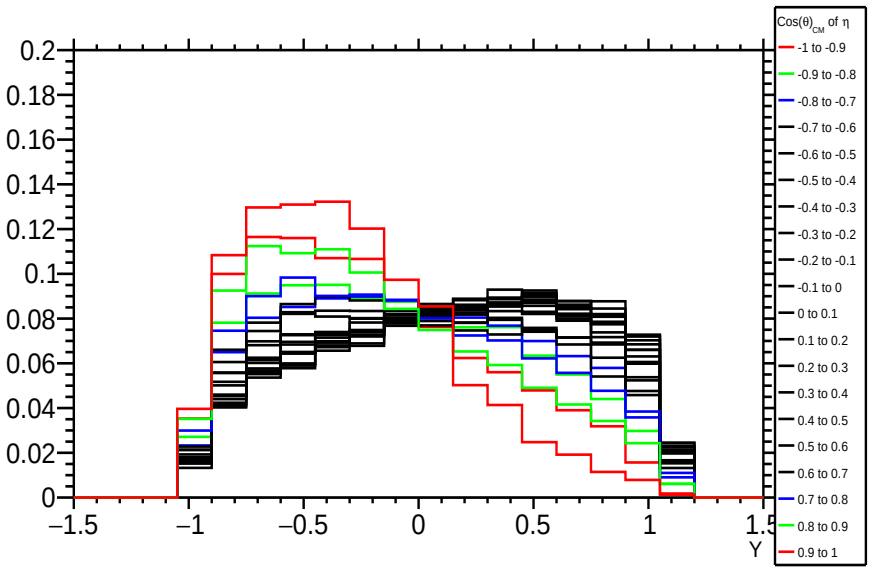

FIGURE 8. Dalitz Variable Y distribution normalised to 1 in each 0.1 bins of $\cos\theta_{center-of-mass}$ of η from g12 data.

3.7. Timing Cuts on proton, π^+ and π^-

As a post PID improvement of the detected final state particles π^+, π^- and proton, we introduced a vertex timing (t_{vert}) cut of particles in the analysis. The t_{vert}, vertex time is the instant of time the particle left the target. One can calculate it through the information of the TOF detectors as,

$$t_{vert}(TOF) = t_{TOF} - \frac{l_{TOF}}{c\beta}$$

where t_{TOF} and l_{TOF} are the measured time and length of particle in TOF sub detector. Here c is the velocity of light in vacuum and β is the Lorentz factor of the particle calculated by knowing the velocity(v) of particle as $\beta = \frac{v}{c}$. The same vertex timing (t_{vert}) information can also be calculated from the RF-corrected time instant of the photon (t_{photon}) crossing the target center measure by the tagger added with the t_{prop}, which is the propagation time from the center of the target to the track vertex. Given by,

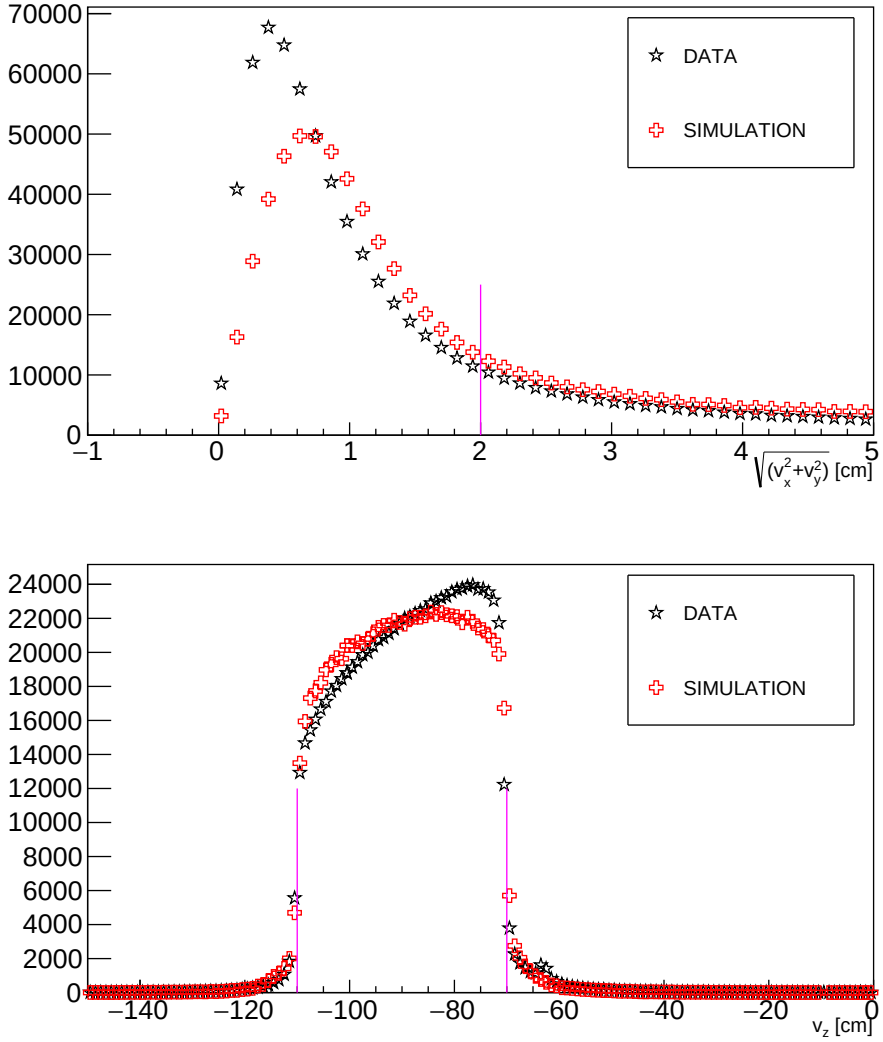

FIGURE 9. [tpho + tprop -scvt] distribution from the simulation and data for proton, π^+ and π^-.

$$t_{vert}(Tagger) = t_{photon} + t_{prop}.$$

The difference of the $t_{vert}(TOF)$ from $t_{vert}(Tagger)$ is shown in Fig. 10, and we make a cut of $\pm$ 1.0 ns around 0 ns for all the final state particles in both simulation and data.

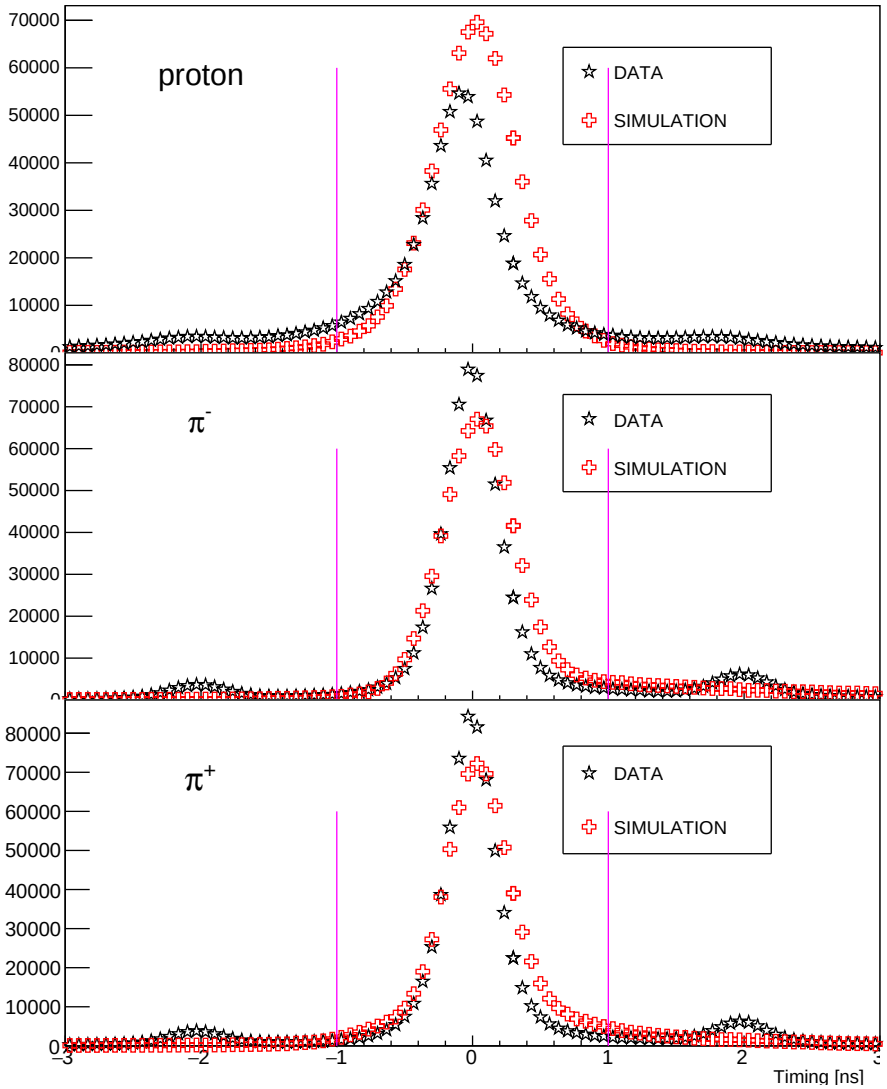

FIGURE 10. $[t_{vert}(TOF)$ - $t_{vert}(Tagger)]$ distribution from the simulation and data for proton(Upper), π^+(Middle) and π^-(Lower).

3.8. Result

The simulated events and g12 data are passed all selection and cuts described in Section. 3.2, Section. 3.6, Section. 3.7, Section. 3.4 and Section. 3.3. The number of the events rejected in both the simulation and data after the cuts is shown in a Table. 3.

In an attempt to see how well the simulation explains the g12 data a comparison of the kinematic variables of the center-of-mass energy ($\sqrt{s}$) and momentum (P), θ and ϕ for

Cuts	g12 Run 56655	Simulation
Generated	—	10001500
Reconstructed	42947	855447
Vertex Cut	20092	505405
Timing Cut	11390	451470
Multiple E_γ	14986	—
Fiducial Cuts	10541	276432
Prob($(\eta)\pi^+\pi^-$p) >0.01	1901	259136

TABLE 3. The table shows the cut flow of the analysis from g12 data run 56655 and simulated events.

π^+ π^- and p is shown in the Figure. 11, 12, 13 & 14. The events in the Monte Carlo are generated with the model explained in Section. 2.2 with the input Dalitz plot parameters from BESIII measurement [2].

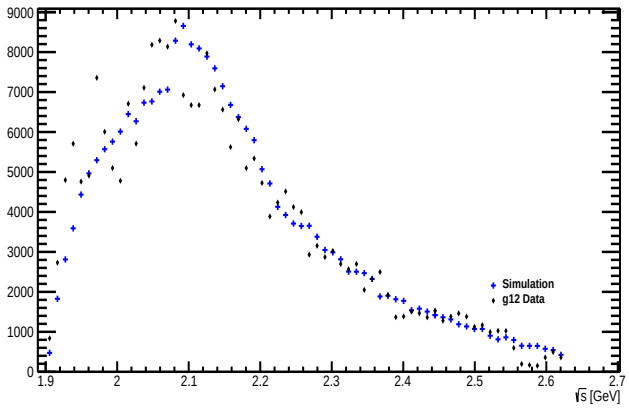

FIGURE 11. Comparison of incident photon beam in center of mass energy ($\sqrt{s}$) with simulated (blue) events and g12 data (black) when generating Monte-Carlo with the differential cross-sections and Dalitz plot parameters.

3.9. Background subtraction to the Dalitz plot

One can also define the boundary of the $\eta' \to \eta\ \pi^+\ \pi^-$ decay from the fact that the addition three momenta of particles $\vec{P}_\eta$, $\vec{P}_{\pi+}$ and $\vec{P}_{\pi-}$ for η, π^+ and π^- respectively is 0

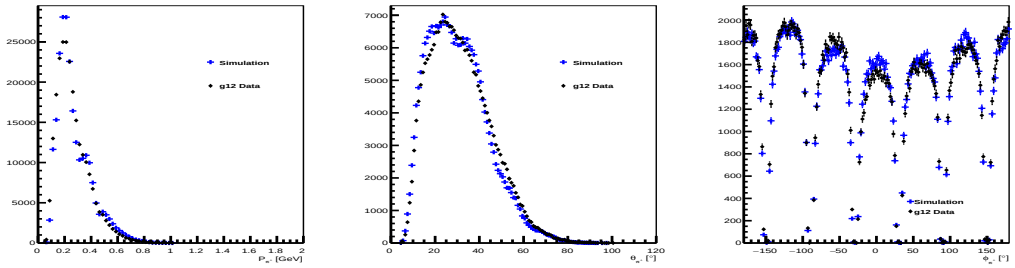

FIGURE 12. Comparison of π^+ momentum (left), π^+ θ (middle) and π^+ ϕ (right) with simulated (blue) events and g12 data (black) when generating Monte-Carlo with the differential cross-sections and Dalitz plot parameters.

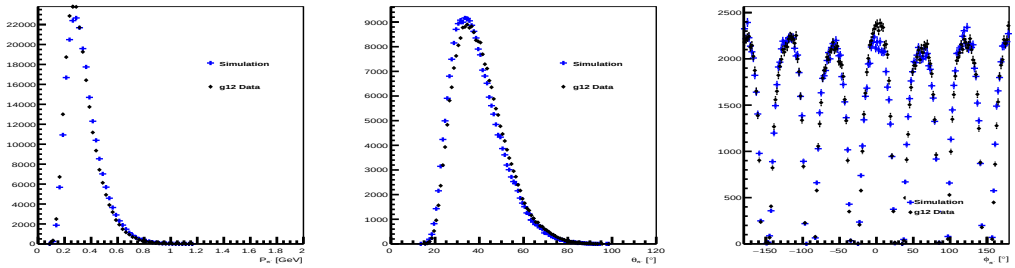

FIGURE 13. Comparison of π^- momentum (left), π^- θ (middle) and π^- ϕ (right) with simulated (blue) events and g12 data (black) when generating Monte-Carlo with the differential cross-sections and Dalitz plot parameters.

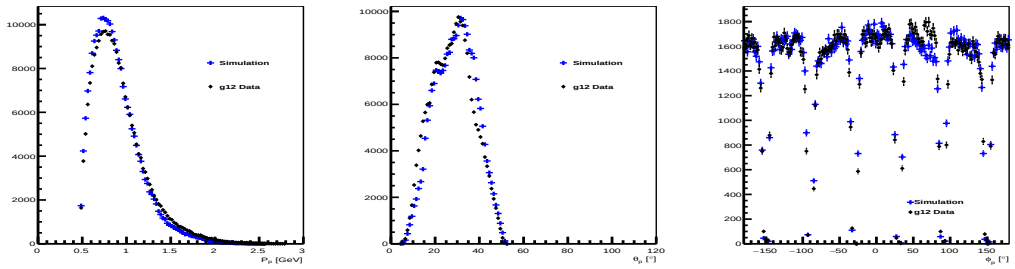

FIGURE 14. Comparison of proton momentum (left), proton θ (middle) and proton ϕ (right) with simulated (blue) events and g12 data (black) when generating Monte-Carlo with the differential cross-sections and Dalitz plot parameters.

in the rest frame of η'.

$$\vec{P}_{\eta} + \vec{P}_{\pi+} + \vec{P}_{\pi-} = 0.$$

Squaring and equating the side gives us the boundary Equation. 4 of the $\eta' \rightarrow \eta\ \pi^+\ \pi^-$ decay.

$$|{P_{\eta}}^2 - {P_{\pi+}}^2 - {P_{\pi-}}^2| \leq 2\vec{P}_{\pi+}.\vec{P}_{\pi-} \tag{4}$$

The aim is now to obtain a bin-wise background subtracted Dalitz plot. In order to achieve that all the events are feed into a X and Y (nbin x nbin) Dalitz plot and a bin-wise background subtraction is performed to the M_x(p) distribution after restricting $0.537 \leq M_x(\mathrm{p}\pi{+}\pi{-}) \leq 0.557$. The signal in M_x(p) distribution is fitted with a Voigt function and background is fitted with a Polynomial of order 3 in each bin of the Dalitz plot to subtract the non-resonant contribution.

One can also translate the 2D Dalitz plot bins of X and Y with a global bin number given by:

$$Globalbin(X,Y) = Floor\big[\frac{X + X_{max}}{\delta}\big] + N_{bins}.Floor\big[\frac{Y + Y_{max}}{\delta}\big] + 1$$

where X and Y are the central values of the current bin, X_{max} and Y_{max} are the maximum values the axis X and Y respectively, which is chosen to be 1.5. The N_{bins} are the number of bins chosen along X and Y axis and it is 15 here. A translation of the Dalitz plot to its Global bin number along with the boundary of the decay from Equation. 4 is shown in Figure. 15.

3.10. Calculation of acceptance with smearing matrix

The CLAS detector has a different acceptance of proton, π^+ and π^- and the acceptance varies within the phasespace of the $\eta' \rightarrow \eta\ \pi^+\ \pi^-$ decay. Hence the migration of events in different bins within the phasespace is also non-uniform, so one must take special care of migration of events from one bin to the other. To take care of the migration of the events, an acceptance with smearing matrix ($\epsilon_{n,m}$) is presented here. The events are generated in each bin of the Dalitz plot and the acceptance for all the bins including

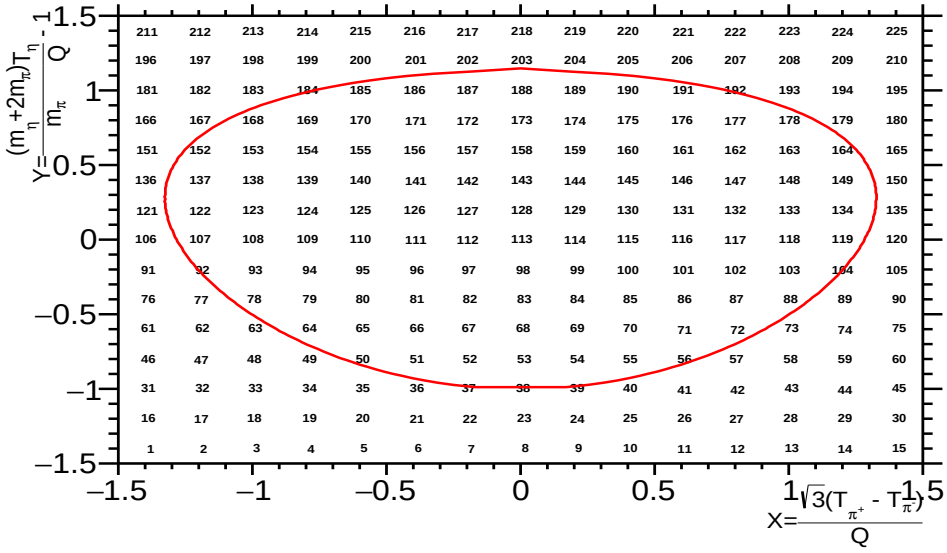

FIGURE 15. The 15 x 15 Dalitz plot shows the translation X and Y Dalitz plot bins in global binning and the red curve shows the phase space boundary of the decay.

the migrated bins are calculated. For events generated in the j^{th} bin, the acceptance is calculated for all i^{th} Dalitz plot bins as shown below :

$$\epsilon_{i,j} = \frac{N_{rec,gen}(i,j)}{N_{gen}(j)} \tag{5}$$

Where $N_{rec,gen}$(i,j) denotes the number of events reconstructed in i^{th} bin when generated events in the j^{th} bin only.

3.11. Fit to the Dalitz Plot

Once the $\eta' \to \eta\ \pi^+\ \pi^-$ events from data is filled in each bin of Dalitz plot. We fit the Dalitz plot with the general parametization function in Equation. 6. The square of the decay amplitude,

$$M^2 = A(1 + aY + bY^2 + cX + dX^2). \tag{6}$$

Where a, b, c, and d are the Dalitz plot parameters of the decay and A is the normalization constant.

The fitting is performed with least square fitting procedure using MINUIT available in ROOT, which minimises the χ^2 using Equation. 7 in each bin of the Dalitz plot.

$$\chi^2 = \sum_{i=1}^{Nbins} \left(\frac{N_i - \sum_{j=1}^{Nbins} \epsilon_{i,j} N_{theory,j}}{\sigma_i} \right)^2 \tag{7}$$

Where,

- The N_i is number of $\eta' \to \eta\ \pi^+\ \pi^-$ events in the i^{th} Dalitz plot bin.
- $\epsilon_{i,j}$ is acceptance with smearing matrix, ie. it gives acceptance of j^{th} bin when events are generated in the ith bin only.
- $N_{theory,j} = \int_{Boundary}$ A(1 + aY + bY^2 + cX + d X^2) dX dY.
- σ_i is the error associated with i^{th} DP bin.

3.11.1. *Phase Space Integrals.* To calculate the integral in Equation. 8, the Monte Carlo integration used within the boundary of the Dalitz plot.

$$N_{theory,j} = \int_{Boundary} A(1 + aY + bY^2 + cX + dX^2) dX dY \tag{8}$$

$$N_{theory,j} = A \int_{Boundary} dX dY + Aa \int_{Boundary} Y dX dY + Ab \int_{Boundary} Y^2 dX dY + Ac \int_{Boundary} X dX dY + Ad \int_{Boundary} X^2 dX dY$$

$$N_{theory,j} = A(\alpha_1 + a\alpha_2 + b\alpha_3 + c\alpha_4 + d\alpha_5)$$

Where,

$\alpha_1 = \int_{Boundary}$ dX dY

$\alpha_2 = \int_{Boundary}$ Y dX dY

$\alpha_3 = \int_{Boundary}$ Y^2 dX dY

$\alpha_4 = \int_{Boundary}$ X dX dY

$\alpha_5 = \int_{Boundary}$ X^2 dX dY

The aim here is to evaluate the integral α_1, α_2, α_3, α_4 and α_5. The uniform random number pair, as Dalitz variable X and Y are generated within -1.5 to 1.5 for both using random number generator in ROOT and saved in a binned two dimensional histogram. If the generated pair lie inside the kinematic boundary of decay then the one binned two

dimensional histogram for each integral is filled, where the integrand being the weight of the histogram. For instance: histogram for integral α_1 is assigned a weight of 1, histogram for integral α_2 is assigned a weight of Y, integral α_3 is assigned a weight of Y^2 so on and so forth. These histograms for each integral is then divided by the generated histogram and multiplied by the bin size to give the value of integration inside the Dalitz plot for each bin. It can be later translated into the global binning and used directly in the Equation. 7.

REFERENCES

[1] V. Dorofeev *et al.*, Phys. Lett. B **651**, 22 (2007)

[2] M. Ablikim *et al.* [BESIII Collaboration], Phys. Rev. D **83**, 012003 (2011)

[3] B. Borasoy and R. Nissler, Eur. Phys. J. A **26**, 383 (2005)

[4] Z. Akbar et al. g12 Analysis Procedures, Statistics and Systematics. Technical report, CLAS Technical Note, 2016.

[5] M. Williams *et al.* [CLAS Collaboration], Phys. Rev. C **80**, 045213 (2009)

[6] Li Caldeira Balkesthl, Measurement of the Dalitz Plot Distribution for $\eta \to \pi^+ \pi^- \pi^0$ with KLOE, PhD thesis Uppsala University 2016.